ELSEVIER

Journal of Nuclear Materials 258–263 (1998) 1902–1907

journal of nuclear materials

Dose dependence of neutron irradiation effects on $MgAl_2O_4$ spinels

A. Ibarra [a,*], D. Bravo [b], M.A. Garcia [c], J. Llopis [c], F.J. Lopez [b], F.A. Garner [d]

[a] *CIEMAT, Inst. Investigación Básica, Euroatom/CIEMAT Association, Avda Complutense, 22, E-28040 Madrid, Spain*
[b] *Departamento de Fisica de Materiales, Facultad de Ciencias (C-IV), Universidad Autonoma de Madrid, Cantoblanco, E-28049 Madrid, Spain*
[c] *Departamento de Fisica de Materiales, Facultad de Ciencias Fisicas, Universidad Complutense de Madrid, 28040 Madrid, Spain*
[d] *Pacific Northwest Laboratory, Richland WA, USA*

Abstract

The characteristics of the photoluminescence and electron paramagnetic resonance (EPR) spectra of stoichiometric $MgAl_2O_4$ spinel specimens irradiated in FFTF-MOTA at temperatures between 385°C and 750°C to fluences ranging from 5.3 to 24.9 × 10^{26} nm^{-2} are measured. Photoluminescence spectra show a complex behaviour associated with the presence of an active defect with different surroundings. The EPR spectra show two different bands that are associated with different defects.

1. Introduction

In recent years interest in the study of irradiation effects on $MgAl_2O_4$ spinels has increased, mainly due to the search for materials with high radiation resistance, for applications in both fusion reactor technology and the nuclear waste industry. In this respect, $MgAl_2O_4$ is one of the ceramic materials with highest radiation resistance, from the point of view of mechanical and elastic properties [1–4]. The reason for this behaviour is not fully understood, but seems to be related to the high concentration of intrinsic defects present in this material. The defects arise mainly from: (a) up to 30% of cation antisite disorder occurs in synthetic crystals, inducing a very high concentration of electron (Al^{3+} in tetrahedral symmetry sites) and hole (Mg^{2+} in octahedral symmetry sites) traps, and (b) $MgAl_2O_4$ crystals always exhibit some deviation from stoichiometry, i.e. the composition is $(MgO)(Al_2O_3)_x$ with $x \geqslant 1$. Thus, cation vacancies are formed to compensate the extra charge of Al^{3+} ions.

After high temperature neutron irradiation it has been observed that the nucleation and growth of defect clusters is greatly inhibited whereas the number of antisite defects increases enormously, in contrast to the response of other oxides [5–7].

Recently, some spinel specimens have been irradiated to a very high dose of neutrons in the FFTF/MOTA reactor at different temperatures to obtain an overall view of the irradiation effects. This present work is a part of a series in which an extensive characterization of these specimens is being made using neutron diffraction [6], optical properties [8,9], and mechanical and elastic properties [3,4]. In particular, we report in this paper the results of a detailed and simultaneous study of the main characteristics of the photoluminescence and electron paramagnetic resonance (EPR) spectra of these samples, including their evolution with increasing neutron dose.

2. Experimental details

The specimens studied were [1 0 0] oriented single crystals, in the form of 4.8 mm diameter cylindrical pellets. The details of impurity levels, specimen fabrication and irradiation are given in Ref. [3]. The neutron irradiations for the specimens studied in this work were performed at three different temperatures: (a) at 385°C, up to a dose of 24.9 × 10^{26} n/m^2 ($E > 0.1$ MeV); (b) at 405°C, up to a dose of 5.3 × 10^{26} n/m^2 ($E > 0.1$ MeV); and (c) at 750°C for 5.6, 13.7 and 21.7 × 10^{26} n/m^2

* Corresponding author. Tel.: +34 1 346 6507; fax: +34 1 346 6068; e-mail: ibarra@ciemat.es.

0022-3115/98/$19.00
PII: S0022-3115(98)00130-5

($E > 0.1$ MeV) doses. After irradiation, thin slices (thickness between 0.2 and 0.5 mm) were cut and polished from the cylinders. The specimens were heated up to 300°C to release all charges trapped in shallow traps. As a general rule, all measurements were performed before and after a small dose X-ray irradiation (up to a dose of 500 Gy) at room temperature, to check the effect of ionizing irradiation and the presence of defects able to trap charge carriers (like F, F^+ or V-centre, see for example Ref. [10]).

EPR spectra were obtained with a Bruker spectrometer model ESP 300E working in the X-band. Accurate values of the microwave frequencies and magnetic fields were obtained with a Hewlett-Packard HP5342A frequency meter and a Bruker ER35 M gaussmeter, respectively. All spectra were measured with a modulation frequency of 100 kHz and a modulation amplitude of 0.5 G.

Photoluminescence measurements were carried out with a fluorescence spectrometer (Perkin Elmer LS-5) fitted with a red sensitive photomultiplier, using a configuration in which the spectra are taken from the illuminated surface, to avoid autoabsorption effects in the excitation spectra. The spectrofluorimeter provides corrected emission and excitation spectra in the 250–720 nm range and in the 230–700 nm range, respectively.

3. Results and discussion

3.1. EPR results

The EPR spectra of irradiated specimens at room temperature typically consist of two bands at $g = 2.0005 \pm 0.0005$ (band A) and $g = 2.083 \pm 0.001$ (band B), see inset of Fig. 1. These bands do not show any dependence on the orientation of the magnetic field with respect to the specimen. Band A is sharp, with a peak-to-peak width of 11 G in the derivative line, whereas band B is 140 G wide. Both bands have not been previously observed in stoichiometric spinel, either for unirradiated specimens or irradiated to lower doses [11]. A sharp band at $g = 2.0016$ (similar to band A) has been observed in $MgAl_2O_4$ spinels with strong deviations from stoichiometry. This band has been attributed to the presence of F^+ centres of cubic symmetry [12].

Band A appears in all the neutron irradiated specimens, whereas band B is only clearly observed in neutron irradiated specimens at the highest temperatures and doses. Fig. 2 shows the obtained dose dependence. It can be observed that band A decreases with increasing dose, and the decrease depends very slightly on temperature, whereas band B weakly increases with dose. This different behaviour suggests that each band is associated with a different kind of defect. This result is further confirmed by the microwave power dependence of band intensities, shown in Fig. 1, where band A saturates at very low power levels, whereas band 2 shows a linear behaviour up to the maximum applied power level.

High dose irradiations of insulator materials (oxides, halides, etc.) at high temperatures usually give rise to the growth of extended defects like dislocation loops, and the formation of metallic colloids. The colloids can be in principle identified by EPR spectroscopy because they induce a sharp band near $g = 2.0023$ (the value for free electrons) associated with the movement of conduction electrons in the metallic particle. The peak position and width of the band depends on the material, as well as on the size and shape of the colloid [13]. For specimen

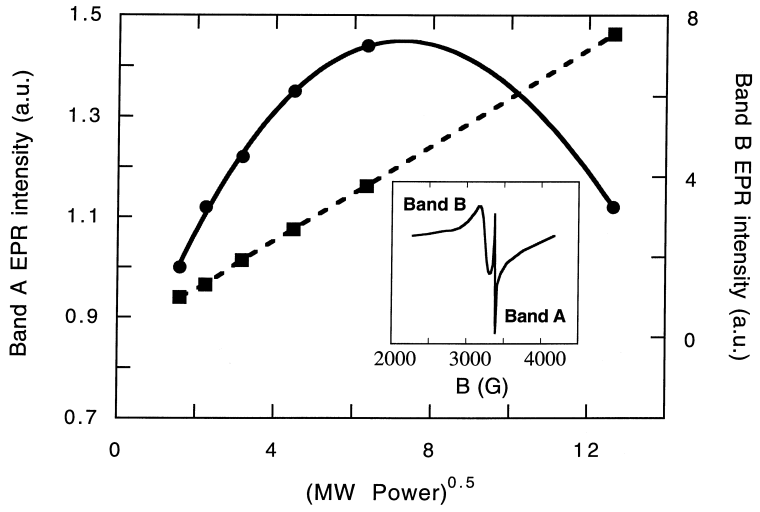

Fig. 1. Microwave power dependence of the two EPR bands observed in neutron irradiated $MgAl_2O_4$ specimens measured in this work: (●) band A and (■) band B. Inset: Typical EPR spectrum for these specimens.

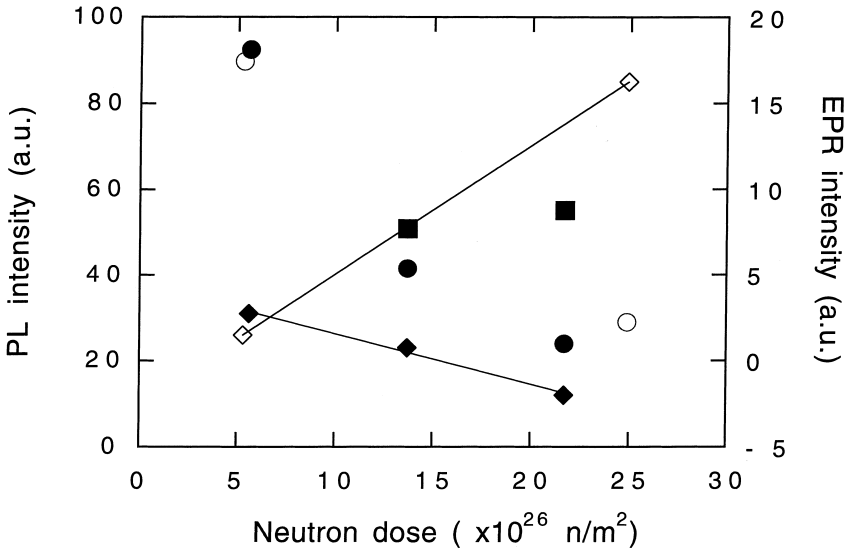

Fig. 2. Dose dependence of the photoluminescence and EPR spectra of specimens irradiated at 750°C (full symbols) and around 385–400°C (open symbols). (♦) photoluminescence emission at about 2.00 eV, (●) EPR band A and (■) EPR band B. Lines are guides for the photoluminescence data.

thicknesses of the order of the skin depth (a few microns) the colloid line is expected to show an asymmetrical shape (Dysonian shape), and the intensity should be essentially independent of temperature (as observed for Van Vleck paramagnetism). For ionic materials the presence of colloids is easily observed after high dose electron irradiation. Therefore, it seems possible that band A could be associated with the presence of colloids in these specimens. To check this, the temperature dependence of the EPR spectra has been measured at 100 and 300 K. No change of position and sharpness of any band was observed. The temperature effect is just a change of the intensity of the bands, with band A a factor 1.90 higher at the lower temperature, whereas the factor for band B is only 1.3. This result suggests that neither of these bands are related to colloids. Instead we believe that band A is due to F^+ centres, similar to the proposal made by Gritsyna and co-workers in Ref. [12].

An additional effect is observed in these specimens. After X-ray irradiation no change of the spectra was found. This is a very interesting result because before neutron irradiation, X-ray irradiation gives rise to a very characteristic and intense EPR spectrum associated with the trapping of holes in cation vacancies (V-centres) [14]. The lack of this band in the EPR spectra of neutron irradiated specimens should indicate that there are no cation vacancies available, although this is unlikely taking into account that their concentration is very high even in the starting material, or that these vacancies are distorted in such a way that they cannot stabilize the holes at the cation sites.

3.2. Photoluminescence results

In previous works performed using the same specimens [8,9] some preliminary results showing two intense emission bands around 1.7–2.0 eV were presented. The relative intensity of both bands, as well as the excitation spectra, appeared to be dependent on the specimen being examined. The detailed study of the photoluminescence spectra made in this work has revealed a much more complex behaviour than initially presented in the earlier work.

Emission photoluminescence spectra are composed of a band centred at about 2.00 eV under excitation with 2.53 eV photon energy, in agreement with the results obtained in Ref. [9]. However, the shape and position of the band is slightly different for each specimen. In particular, the maximum emission for the specimen irradiated to 21.7×10^{26} n/m^2 at 750°C is at 2.06 eV, and at 1.94 eV for that irradiated to 5.6×10^{26} n/cm^2 at 750°C, whereas all the other specimens peak in between. It was found that the peak of this emission band shifts toward a high energy range with increasing irradiation dose.

An important point is that, for each specimen, the peak position of the emission spectrum changes with the photon energy excitation. The inset in Fig. 3, showing the emission spectra for three different excitation photon energies, illustrates this effect for the specimen irradiated to 24.9×10^{26} n/m^2 at 385°C. Fig. 3 summarizes the results obtained for all the specimens showing the peak position of the emission spectra as a function of excitation photon energy. A linear shift of the maximum is clearly observed. In this figure it can also be observed

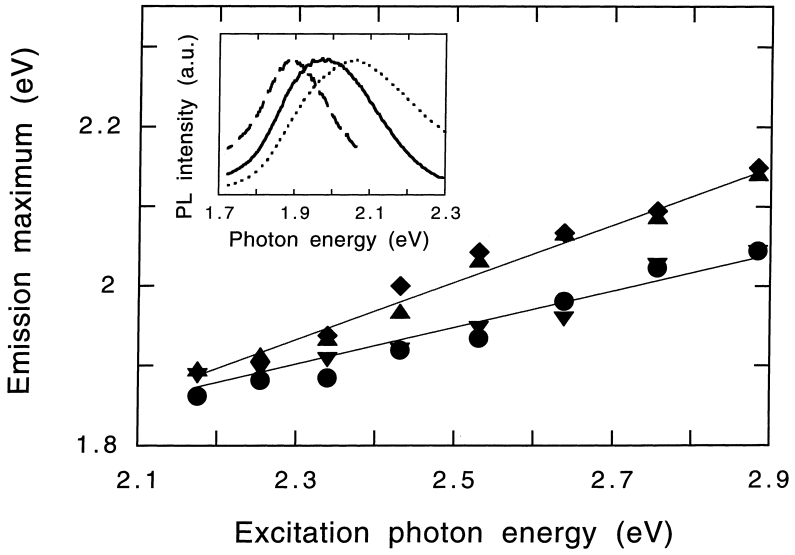

Fig. 3. Peak position of the emission spectra as a function of the excitation photon energy for the specimen (●) irradiated to 5.6×10^{26} n/m^2 at 750°C, (▼) 5.3×10^{26} n/m^2 at 405°C, (▲) 24.9×10^{26} n/m^2 at 385°C, and (♦) 21.7×10^{26} n/m^2 at 750°C. Inset: Photoluminescence emission spectra of sample irradiated up to 5.6×10^{26} n/m^2 at 750°C, exciting with photon energies of (—— ——) 2.17 eV, (———) 2.43 eV and (- - - - -) 2.64 eV.

that for a given excitation photon energy, the position of the peak for the emission spectra is higher for the specimens with higher neutron dose whereas no clear effect of irradiation temperature appears. No effect associated with the measuring temperature was observed.

The excitation spectrum exhibits a broad band centred around 2.6 eV. Also, slight differences can be observed among excitation spectra of different samples, but again, the main point is that the shape and peak position of the spectra is dependent on the photon energy of the monitored emission. The inset in Fig. 4 illustrates the changes in the excitation spectrum at different emission photon energies for specimen irradiated to 5.6×10^{26} n/m^2 at 750°C. Fig. 4 summarizes this behaviour for different specimens. In this case, no linear shift is observed, but the spectra show a step structure, with no clear effect of irradiation temperature or dose on the results. This behaviour suggests that the excitation spectra for all the specimens consist of at least two different excitation bands at approximately 2.4 and 2.6 eV.

This complex behaviour of the excitation and emission spectra can be understood assuming that the photoluminescence can be related to a single defect type with various distorted surroundings.

In addition, Fig. 2 shows the dose dependence of the photoluminescence intensity for different specimens. It is interesting to note that the photoluminescence intensity increases with dose for specimens neutron irradiated at low temperature, whereas it decreases with dose for those irradiated at high temperature. This behaviour is completely different to that observed in the EPR spectra, indicating that these measurements may be associated with different type of defects.

3.3. Correlation with optical absorption spectra

In a previous report [8] detailed measurements of the optical absorption spectra of these specimens were presented. It was shown that irradiation induces an increase of the optical absorption in the whole ultraviolet range, together with an absorption band peaking at about 2.48 eV. In an effort to establish correlations among the data from different measurement techniques, the optical absorption spectra presented in Ref. [8] have been decomposed into different components and their dose evolution obtained. In the ultraviolet range, it is known that $MgAl_2O_4$ spinels show strong absorption bands associated with different defects (for example, 4.77 and 5.28 eV related to F^+ and F centres respectively [15]). Thus, the strong ultraviolet absorption observed in these specimens has been associated with an exponential shape component, as this function is a good fit to the lower part of a very intense absorption band, a gaussian band centred around 2.42 eV, with a halfwidth of 0.19 eV, and a residual band. This residual band has a complex structure around 2.48 eV, and has a very similar shape for all the specimens. It was found that the dose dependence of the gaussian component is similar to that observed for the photoluminescence. This indicates they likely have the same origin. This is further confirmed by comparison of optical absorption and photoluminescence spectra, by which the similarities between them are

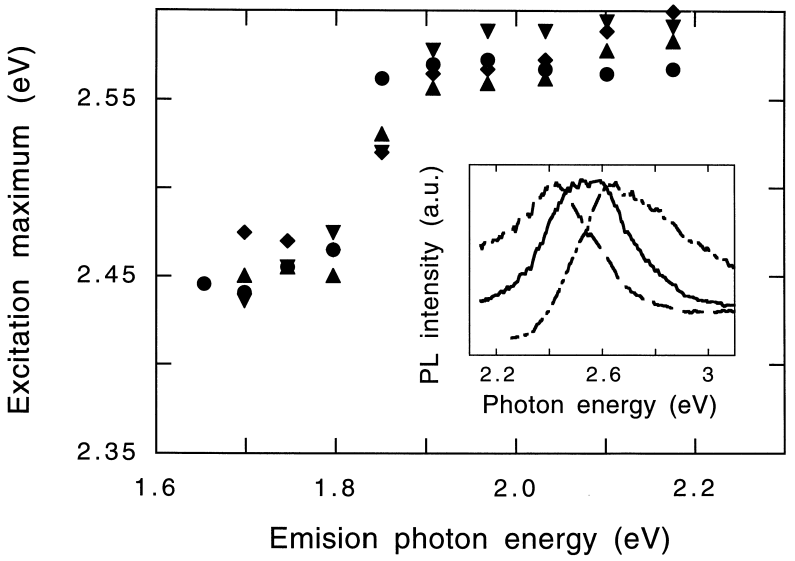

Fig. 4. Peak position of the excitation spectra as a function of the emission photon energy for the specimen (●) irradiated to 5.6×10^{26} n/m^2 at 750°C, (▼) 5.3×10^{26} n/m^2 at 405°C, (▲) 24.9×10^{26} n/m^2 at 385°C, and (♦) 21.7×10^{26} n/m^2 at 750°C. Inset: photoluminescence excitation spectra of specimen irradiated to 5.6×10^{26} n/m^2 at 385°C for emission photon energies of (—— ——) 1.65 eV, (———) 1.91 eV and (—— - ——) 2.17 eV.

clearly observed. No other correlation is found between optical absorption and other measuring techniques.

4. Conclusions

The EPR and photoluminescence characteristics of different irradiated specimens have been studied with emphasis on the effects of displacement dose and irradiation temperature. It has been found that no correlation appears between the EPR, photoluminescence and optical spectra, except for optical absorption peak at 2.42 eV, and the photoluminescence intensity. The photoluminescence spectra show a complex behaviour that may be related to the presence of a defect with different and distorted surroundings. For the highest temperature irradiation, most of the observed effects decrease with dose, whereas in the low temperature irradiation the EPR bands decrease and the photoluminescence spectra increase strongly with dose. It has been concluded also that the EPR characteristics are probably not related to the presence of colloids in the specimens, but arise due to F^+ defects.

Acknowledgements

This work was performed in the framework of CIEMAT projects for Nuclear Fusion Research and was partly supported by European Union within the European Fusion Technology Programme and by the CYCIT (Spain) under contract numbers PB92-1081-C02-01 and PB93-0428. The neutron irradiation and the participation of F.A. Garner was supported by the US Department of Energy, Office of Fusion Energy.

References

[1] F.W. Clinard Jr., G.F. Hurley, L.W. Hobbs, J. Nucl. Mater. 108&109 (1982) 655.
[2] F.W. Clinard Jr., G.F. Hurley, R.A. Youngman, L.W. Hobbs, J. Nucl. Mater. 133&134 (1985) 701.
[3] F.A. Garner, G.W. Hollenberg, F.D. Hobbs, J.L. Ryan, Z. Li, C.A. Black, R.C. Bradt, J. Nucl. Mater. 212–215 (1994) 1087.
[4] C.A. Black, F.A. Garner, R.C. Bradt, J. Nucl. Mater. 212–215 (1994) 1096.
[5] K. Fukumoto, C. Kinoshita, S. Maeda, K. Nakai, Nucl. Instr. and Meth. B 91 (1994) 252.
[6] K.E. Sickafus, A.C. Larson, N. Yu, M. Nastasi, G.W. Hollenberg, F.A. Garner, R.C. Bradt, J. Nucl. Mater. 219 (1995) 128.
[7] K.E. Sickafus, N. Yu, M. Nastasi, Nucl. Instr. and Meth. B 116 (1996) 85.
[8] A. Ibarra, R. Vila, F.A. Garner, J. Nucl. Mater. 233–237 (1996) 1336.
[9] A. Ibarra, F.A. Garner, G.L. Hollenberg, J. Nucl. Mater. 219 (1995) 135.

[10] P.W. Levy, Phys. Rev. 123 (1961) 1226.
[11] A. Ibarra, D. Bravo, F.J. Lopez, I. Sildos, Mater. Sci. Forum 239–241 (1997) 595.
[12] V.T. Gritsyna, V.A. Kabyakov, Sov. Phys. Tech. Phys. 30 (1985) 206.
[13] A.E. Hughes, S.C. Jain, Adv. Phys. 28 (1979) 717.
[14] A. Ibarra, F.J. Lopez, M. Jiminez de Castro, Phys. Rev. B 44 (1991) 7256.
[15] L.S. Cain, G.J. Pogatshnik, Y. Chen, Phys. Rev. B 37 (1988) 2645.